Calculation of Steady Flow About Propellers Using a Surface Panel Method

John L. Hess* and Walter O. Valarezo†
Douglas Aircraft Company, Long Beach, California

A general method for making detailed calculations of flow about propellers with centerbodies has been constructed by adapting a surface panel method. Apparently this is the first method capable of obtaining reliable surface pressure distributions in the blade leading-edge region. New features of the program include input of an axisymmetric nonuniform onset flow, provision for blade symmetry, and generation of the helical wake, including a special far-wake approximation. Calculated blade pressure distributions for a ship propeller and propeller efficiencies for an aircraft propeller agree well with experimental data. Several sample calculations have been included.

Nomenclature

C_p, C_T, C_Q	= pressure, thrust, and torque coefficients, respectively
J	= advance ratio, $= U_\infty/2nR$ or $\pi U_\infty/\omega R$
L	= axial extent of vortex filament wake
M	= number of wake segments
N	= number of panels on one blade plus nonredundant portion of hub
NB	= number of blades
$N\theta$	= number of circumferential increments on nonredundant portion of hub
n	= revolutions per unit time
R	= radius of tip of blade
r	= radial coordinate from axis of rotation
r_{TE}	= r at a trailing-edge point from which a helical vortex issues
$\mathbf{r}$	= vector between two points in space
U_∞	= freestream velocity
V	= velocity magnitude
x,y,z	= Cartesian coordinates fixed in blade
x,r,θ	= cylindrical coordinates fixed in blade
β	= helix angle of vortex filament
Γ	= circulation around a blade section
η	= propeller efficiency
ρ	= fluid density
ω	= circular frequency, $= 2\pi n$

Subscripts

i	= quantities for ith panel

Introduction

SURFACE panel methods for calculating low-speed flow are now so commonly used in all types of design that a detailed description of one is superfluous. Accordingly, only the briefest account is presented here to mention certain aspects that required modification for the propeller application.

The surface of the body about which flow is to be computed is approximated by a large number of small flat quadrilateral panels, as shown in Fig. 1. These panels are on the actual surface of the body, as opposed to an interior plane or "camber surface," which is used by vortex-lattice or lifting-surface methods. It is this feature of a surface panel method that enables it to calculate numerically exact solutions, including detailed surface pressure distributions. For example, at the leading edge of a wing or blade the camber surface vorticity sheet simply terminates at nonzero strength, which yields a $-\infty$ pressure. The finer the lattice subdivisions are made, the more closely this singularity is approximated. In practice, this peak is suppressed by some arbitrary adjustment. By contrast, a surface panel method represents the rounded shape of the leading edge and becomes more accurate as the panel number increases.

Fluid dynamic singularities, source and dipole or vorticity, are placed on each panel and their strengths adjusted to satisfy the boundary conditions. Different panel methods carry this out in various ways. The one used here[1] uses a source density on all on-body (as opposed to wake) panels and, in addition, uses a dipole density on panels contained in those portions of the body designated as lifting. For this purpose, a lifting portion of a body is defined as one having a trailing edge along which a Kutta condition is applied and from which a trailing vortex wake issues (Fig. 1). Previously,[1] this wake was also represented by dipole panels, but that has been replaced in the present work by concentrated vortex filaments. The source strengths are considered independent, but the dipole and vortex strengths are associated in such a way that there is a single value for each "lifting strip" of panels that lies upstream of each trailing-edge segment, including the associated wake vorticity.

On each panel, a centrally located control point is chosen where the zero normal-velocity boundary condition is to be applied and where surface velocities and pressures are eventually calculated. If there are N panels on the body, the set of velocities at the control points due to the source densities form an $N \times N$ matrix of aerodynamic influence coefficients. Taking normal components gives the coefficient matrix for a set of linear equations that expresses the normal-velocity boundary condition. Flow solutions are obtained using a direct matrix solution for a set of onset flows consisting of the flow from infinity and each of the dipole onset flows described previously. These flow solutions are combined in such a way that the Kutta condition is satisfied at all trailing-edge segments to produce a single final solution.

In principle, a surface panel method can calculate flow about any body, including a propeller, and in this sense the problem has been solved for many years. As a practical matter, such an application would prove quite cumbersome, and, in fact, appears never to have been done. To the

Presented as Paper 85-0283 at the AIAA 23rd Aerospace Sciences Meeting, Reno, NV, Jan. 14-17, 1985; received Feb. 14, 1985.

*Principal Staff Engineer.
†Engineer/Scientist. Member AIAA.

N.B.: This work was sponsored by the Naval Ocean System Center, San Diego, CA.

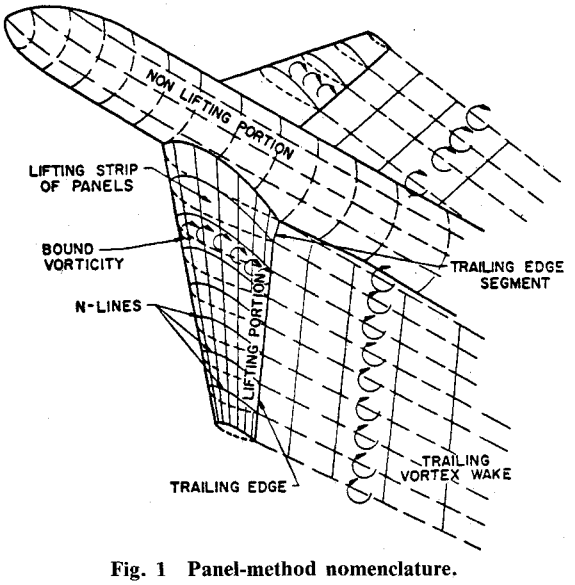

Fig. 1 Panel-method nomenclature.

authors' knowledge, the present work is the first application of a surface panel method to propellers and, thus, the first to obtain reliable pressure distributions, particularly near the leading edge of the blade.

If a propeller is immersed in an axisymmetric flowfield whose symmetry axis is identical with the propeller's axis of rotation, the flow is independent of time in a coordinate system fixed in the blades. Clearly this includes the case of a uniform stream parallel to the propeller axis. For any other flow, e.g., an inclined uniform stream or a nonaxisymmetric flowfield due to another body, the flow in blade-fixed coordinates is time harmonic. Only the steady case has been done, and that is the subject of this paper. However, it was intended from the outset to address the time-harmonic case. While this work remains to be done, the intention to include it has led to certain decisions concerning the numerical approach that might have been made differently if the steady case were the only one of interest.

Producing a usable propeller code basically meant automating those portions of the propeller problem that are so awkward to input to the ordinary panel method.[1] The resulting code is easier to apply to propellers with hubs than the basic panel method is to wing fuselages. The three main features are the provision for any number of blades, the generation of the hub panels, and the generation of the wake vortex filaments. These features are required for any propeller, aircraft or marine. In addition, a special feature has been added to the program allowing input of a special kind of nonuniform onset flow characteristic of that incident to a torpedo propeller.

Provision for any Number of Blades

The principal geometric inputs to the program are the coordinates of a set of points defining one of the blades. Panels are generated from these points in the usual way. The other geometric input consists of points defining the profile curve of the hub. This may be anything from a constant-diameter cylinder to a complete axisymmetric body on which the propeller is mounted, e.g., a torpedo. For a given blade number NB, the hub-generating routine divides the nonredundant part of the hub into $N\theta$ increments equally spaced in circumferential angle. The points defining the hub profile curve are rotated successively by these angular increments to produce hub defining points that are then used to generate panels. The nonredundant portion of the hub subtends a circumferential angle of $2\pi/NB$ on the portions upstream and downstream of the blade. Over the axial location of the blades the nonredundant portion of the hub subtends a somewhat smaller angle due to the finite blade thickness.

The usual panel-method formulas are used to calculate the $N\times N$ matrix of aerodynamic influence coefficients that expresses the effects of the panels on the input blade and nonredundant hub portion at their own control points. These panels are then rotated an angle $2\pi/NB$ about the propeller axis; the effects of these rotated panels are calculated at the control points of the input blade and nonredundant hub portion. This process is repeated until all blades have been accounted for. The result is NB real $N\times N$ matrices. In the steady case the singularity strengths at corresponding panels of the various blades and hub portions are equal. Thus the $N\times N$ real matrix used in the calculations is just the sum of the above matrices. In the time-harmonic case the singularity strengths on corresponding panels all have equal complex absolute values but differ in complex argument by an amount depending on the circumferential location of the blade and the particular harmonic considered. Thus, before they are added, each of the preceding matrices are multiplied by a complex phase shift. The result is a set of $N\times N$ complex matrices—one for each harmonic. This very natural way of handling the time-harmonic case is the reason the present procedure, which uses the same panel distribution on all blades, was chosen. The use of reduced panel densities on the rotated blades[2] saves some computer time, but this is estimated to be only a 20% saving in the steady case and an utterly negligible saving in the time-harmonic case.

The Helical Wake

Originally, it had been planned to provide for an initial nonhelical portion of the wake immediately downstream of the blade to be input by the user. This is now considered to be future work, and the vortex filaments in the wake are taken as helices right from the trailing edge. Thus, the wakes employed correspond to the case of lightly loaded propellers. A first approximation to the effects of moderate loading can be obtained by increasing the helix angle β to a larger value than the one that corresponds to the particular advance ratio being considered in the lightly loaded case. Provision has been made to input these angles.

Helical vortex filaments issue from the edges of the lifting strips at the trailing edge (N-lines in Fig. 1). Let r_{TE} be the radical distance from the axis of rotation of a point from which a helical vortex issues. The axis of rotation is taken as the x axis. Let J be the advance ratio and U_∞ the freestream velocity. The circular frequency of rotation ω is then given by

$$\omega = \pi U_\infty / JR \tag{1}$$

where R is the radius of the blade tip. As mentioned previously, the helix angle β may be input for each radial location. Alternatively, it is calculated from

$$\tan\beta = U_\infty / \omega r_{TE} \tag{2}$$

In either case define

$$p = 1/r_{TE}\tan\beta \tag{3}$$

To generate the helix the number of wake segments M is specified. The x distribution of points on the helix is then governed by three geometric quantities, two of which are input from which the other is calculated. These are: Δ/r_{TE}, where Δ is the x length of the first wake segment; L/r_{TE}, where L is the total x length of the wake; and growth factor ρ. They are related by

$$L = \Delta\frac{\rho^M - 1}{\rho - 1}, \qquad \rho > 1$$

$$= M\Delta, \qquad \rho = 1 \tag{4}$$

The two lengths Δ and L are input as ratios to r_{TE}. The x coordinates of the wake points are

$$x_k = x_{k-1} + \delta x_k, \qquad k = 1,2,\ldots,M$$

$$\delta x_k = \rho^{k-1}\Delta, \qquad x_0 = x_{TE} \tag{5}$$

The corresponding y and z coordinates are

$$y_k = y_{k-1}\cos(p\delta x_k) - z_{k-1}\sin(p\delta x_k)$$

$$z_k = y_{k-1}\cos(p\delta x_k) + y_{k-1}\sin(p\delta x_k)$$

$$y_0 = y_{TE}, \qquad z_0 = z_{TE} \tag{6}$$

Constant-strength straight-line vortices connect successive points. The velocity due to such a vortex at a point (x,y,z) is

$$V_k = \frac{r_{k-1} \times r_k}{r_{k-1}r_k + r_{k-1} \cdot r_k}\left(\frac{1}{r_{k-1}} + \frac{1}{r_k}\right) \tag{7}$$

where

$$r_k = (x-x_k)i + (y-y_k)j + (z-z_k)k$$

$$r_k = |r_k| \tag{8}$$

The line vortex is rotated about the propeller axis by successive angles of $2\pi/NB$, the calculation is repeated, and the results added. Similarly, the results are added for all segments of the helix.

There is a helical vortex starting at the trailing edges of both of the N lines that border a lifting strip. Since these represent the two legs of a semi-infinite "horseshoe" vortex, the vorticity has an opposite sense on the two helices. To complete the "horseshoe" vortex, a line vortex of the same strength as the two helical vortices is placed along the trailing edge of the strip with the vorticity vector pointing from the trailing edge of the first edge to that of the second. Its effect is calculated from an expression of the form of Eq. (7). As in the ordinary panel method,[1] a lift "carryover" is used from the blade-hub intersection to the axis of rotation. The trailing "hub vortex" lying along the axis is straight, and its effect may be evaluated analytically.

The Far-Wake Approximation

Since the helical vortices issuing from the strip trailing edges are semi-infinite, the numerical problem is to approximate their effects at the control points as accurately as possible with a minimum of computational effort. The most straightforward procedure is to extend these vortices a sufficient distance downstream so that further extension does not appreciably change the velocity induced at the control points. Unfortunately the necessary termination distance is rather large, and the number of straight-line vortices involved is also large because each turn of the helix must be well represented and because helices trail back from all blades. Accordingly, a means had to be found for shortening the distance at which the numerical integration of the helix could be terminated.

The scheme that has been adopted is to replace the helical vortex and its rotations at each radial location by the semi-infinite cylindrical wake of an infinitely-many-bladed propeller downstream of some axial location. It seemed likely that use of this downstream approximation, rather than simply ignoring the downstream portion of the wake, would permit much earlier termination of the time-consuming numerical integration. Such turned out to be the case. Numerical experimentation indicated that very good accuracy was obtained if the numerical integration was carried even a short distance downstream. For example, the wakes from the three-bladed propeller of Fig. 7 extended downstream only one-half of a local radius. Increasing this to 1.5 radii changed the load distributions in the fourth significant figure. For larger blade numbers, the approximation should be even better. Moreover, 22 straight-line vortices gave sufficient accuracy for the advance ratios considered, although possibly this point deserves further study. The advantage of this approach is that the entire semi-infinite extent of the helical vortices on all blades is replaced by a small number of closed-form analytic expressions, for which the total computation time is equal to that of only a few straight-line vortices.

Let the cylindrical wake have a radius r_0 and begin at an axial location x_0. Let the control point, where induced velocity is being evaluated, have axial location x and radial location r. Define the quantities

$$q = 1 + \frac{(x-x_0)^2 + (r-r_0)^2}{2rr_0}$$

$$s = \sin^{-1}\left(\frac{x-x_0}{\sqrt{(x-x_0)^2 + (r-r_0)^2}}\right)$$

$$t = \frac{\sqrt{4rr_0}}{\sqrt{(x-x_0)^2 + (r+r_0)^2}} \tag{9}$$

and the function

$$K_1 = \pi + \frac{x-x_0}{2\sqrt{rr_0}}Q_{-1/2}(q) + \frac{\pi}{2}\Lambda_0(s,t), \qquad r \le r_0$$

$$= \frac{x-x_0}{2\sqrt{rr_0}}Q_{-1/2}(q) - \frac{\pi}{2}\Lambda_0(s,t), \qquad r \ge r_0 \tag{10}$$

In Eq. (10), Q is the Legendre function of the second kind and Λ_0 is Neumann's Lambda function.[3] Finally, define a function K_2 that is the same as K_1 with the r inequalities reversed. Then the cylindrical components of velocity at the point are

$$V_x = -\frac{L(\text{total})\,NB}{\pi r_0 \tan\beta}K_1$$

$$V_r = \frac{L(\text{total})NB}{\pi\sqrt{rr_0}\tan\beta}Q_{1/2}$$

$$V_\theta = -\frac{L(\text{total})NB}{\pi r}K_2 \tag{11}$$

These are reduced to Cartesian velocity components in the standard manner. Derivation of the above results is contained in Ref. 4.

Pressure and Force Calculation

The machinery of the preceding sections is used with the panel method to calculate velocity vectors V_i and magnitudes V_i at the control points. From these a pressure coefficient C_p is calculated from

$$C_{p_i} = 1 - (1/U_\infty^2)(V_i^2 - r^2\omega^2) \tag{12}$$

where r is the radial location of the point in question. The pressures in Eq. (12) have been normalized with respect to freestream dynamic pressure $\frac{1}{2}\rho U_\infty^2$. This is proper when summing for forces and moments. However, the blade sections experience local onset flow velocities higher than freestream, and use of Eq. (12) gives larger values of C_p both positively and negatively than are usually encountered. To render the results more conventional, the pressures should be normalized with respect to a local dynamic pressure

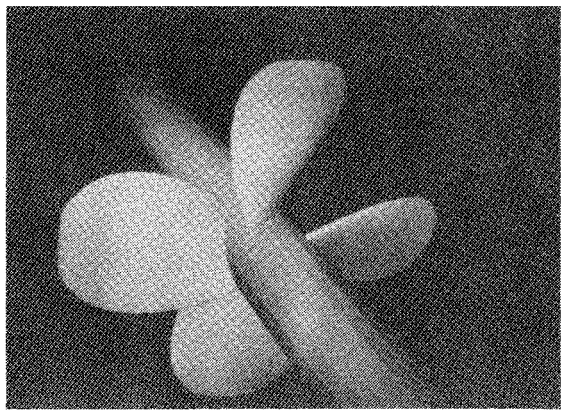

Fig. 2 Ship propeller.

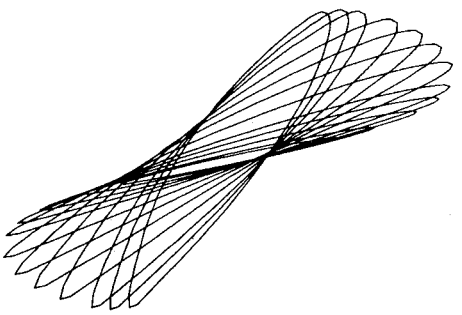

Fig. 3 Blade sections for the ship propeller.

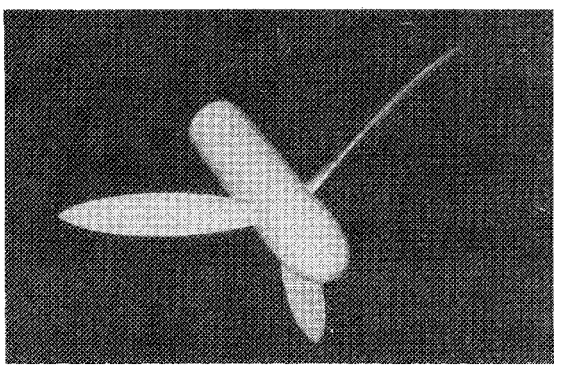

Fig. 4 Aircraft propeller.

$\frac{1}{2}\rho(U_\infty^2 + r^2\omega^2)$. This yields a pressure coefficient

$$C_{p_i}(\text{local}) = \frac{C_{p_i}}{[1 + \pi^2 r^2 / J^2 R^2]} \tag{13}$$

Integrated thrust and torque coefficients are

$$C_T = \frac{J^2}{8} \frac{NB}{R^2} \sum_i A_i C_{p_i} n_{ix}$$

$$C_Q = \frac{J^2}{16} \frac{NB}{R^3} \sum_i A_i C_{p_i} (n_{iy} z_i - n_{iz} y_i) \tag{14}$$

where x_i, y_i, z_i, n_{ix}, n_{iy}, n_{iz}, and A_i are, respectively, control point coordinates, unit normal vector components, and area for the ith panel. These sums can be performed separately over blades and hub.

The propeller efficiency η is

$$\eta = \frac{J}{2\pi} \frac{C_T}{C_Q} \tag{15}$$

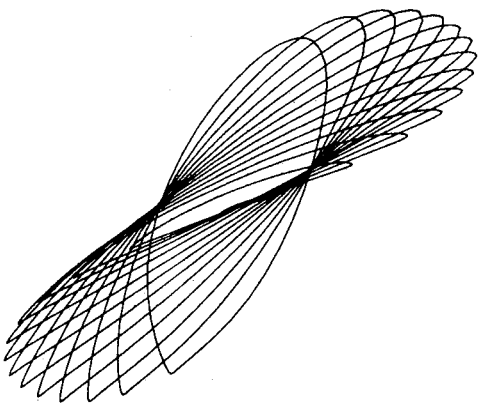

Fig. 5 Blade sections for the aircraft propeller.

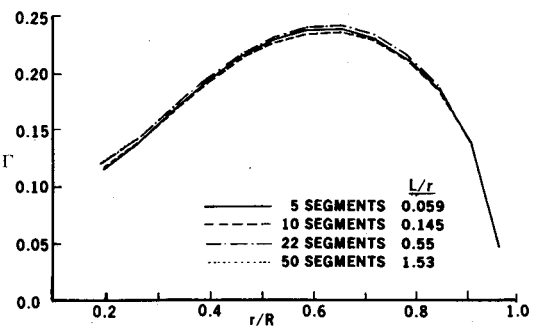

Fig. 6 Radial circulation distributions on the aircraft propeller for various lengths of helical wake.

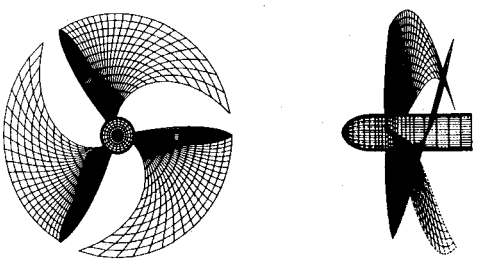

Fig. 7 Twenty-two-segment wake.

Onset Flow to a Torpedo Propeller

Torpedo propellers, mounted as they are on the downstream end of a relatively long body, are immersed in a boundary layer. This is accounted for in the design of so-called "wake-adapted" propellers and results in blades of greatly reduced twist, since the axial velocity is smaller for smaller values of radius. To aid in the design of such propellers, the program accepts as input, the axial, radial, and circumferential components of onset flow velocity, and also total pressure, as functions of radial location in the propeller plane. These are used in the code instead of the uniform onset flow, not only in the normal-velocity boundary condition, but in the default formula for helix angle β and in the calculation of pressure. The velocity field due to the blades is a potential flow. Determination of the physical significance of such a calculation when the onset flow has a variable total pressure is the responsibility of the user.

The Two Propellers Selected as Examples

By way of example, two propellers were selected and calculations were performed for several conditions. These two propellers were selected because some experimental data were available. After comparison of the calculations with these data, further calculations were performed for other conditions to illustrate various features of the method.

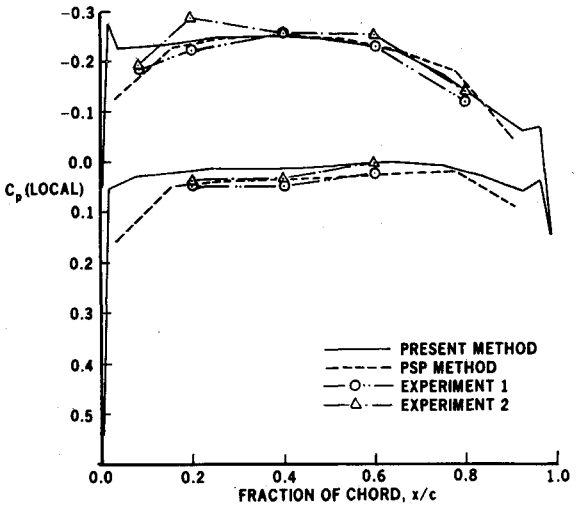

Fig. 8 Pressure distributions on the ship propeller at $r/R=0.7$ for $J=0.402$.

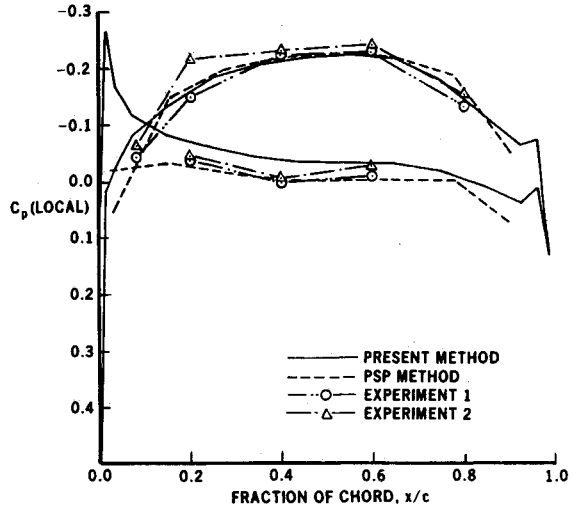

Fig. 9 Pressure distributions on the ship propeller at $r/R=0.7$ for $J=0.603$.

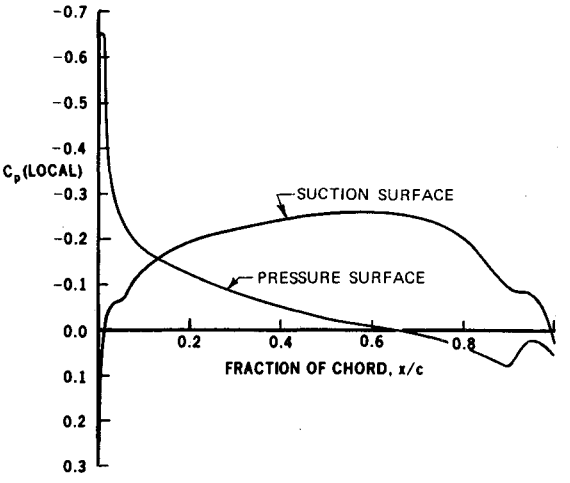

Fig. 10 Two-dimensional pressure distribution on the blade section of the ship propeller at $r/R=0.7$ calculated by a conformal mapping method at an angle of attack corresponding to $J=0.603$.

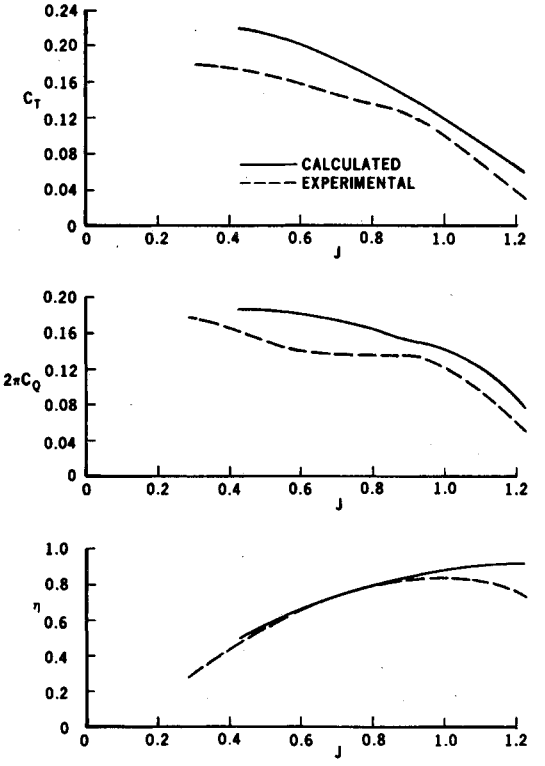

Fig. 11 Thrusts, torques, and efficiencies for the aircraft propeller.

The first propeller is a four-bladed ship propeller. It is shown in Fig. 2 mounted on a cylindrical hub, which was the experimental geometry, but calculations were also performed with the propeller mounted on a body. The blade sections are shown in Fig. 3, where it can be seen that they have rounded trailing edges. The second propeller, which is a three-bladed aircraft propeller, is shown with its hub in Fig. 4, and its blade sections are shown in Fig. 5. The large variation in blade thickness and twist typical of such propellers is clearly evident.

A preliminary series of calculations explored requirements for the lengths of the helical wakes. Surprisingly, it turned out that short wakes were adequate. Figure 6 shows calculated radial circulation distributions for the aircraft propeller at $J=0.9$ using four different wakes of various lengths and a number of vortex segments. The 22-segment wake whose axial length is only one-half of the local helix radius is sufficient. Further increase in wake length or segment number gives results graphically indistinguishable from those of this wake. Figure 7 shows the 22-segment wake and illustrates how short it is both axially and circumferentially. Similar results were obtained from the ship propeller. This illustrates the effectiveness of the far-wake approximation.

Comparison of Calculated and Experimental Results

One of the strengths of a surface panel method is that, unlike other methods, it routinely obtains surface pressure distributions, and these are known to be reliable. Accordingly, comparison of the present calculations with pressure data was a first priority. Fortunately, such comparisons were performed for the ship propeller by Blaisdell.[5] Figures 8 and 9 show pressure distributions normalized with respect to local dynamic pressure for a radial location of 0.7 times the propeller radius at two advance ratios, $J=0.402$ and 0.603. Four pressure distributions are shown: that calculated by the present panel method; two experimental distributions, whose difference is a measure of experimental error; and a distribution calculated by Kim and Kobayashi[6] using a vortex-lattice method,[2] that is labeled the PSP method. All four distributions agree in the midchord region. Discrepancies between the two calculated pressure distributions become dramatic only at the leading edge, where experimental values were not obtained. However, this is just the region where experience has shown that a vortex-lattice method has difficulty but a surface panel method does not. At the design advance ratio, $J=0.402$, the blade sections are operating at the so-called "ideal" angle

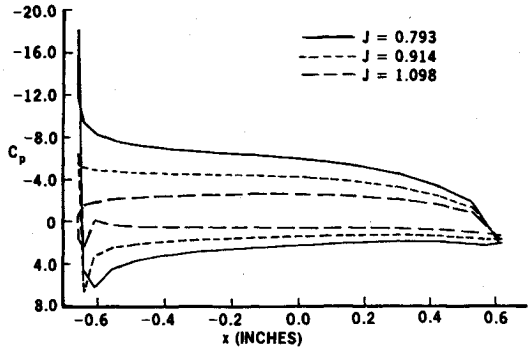

Fig. 12 Calculated pressure distributions on the aircraft propeller at $r/R=0.7$.

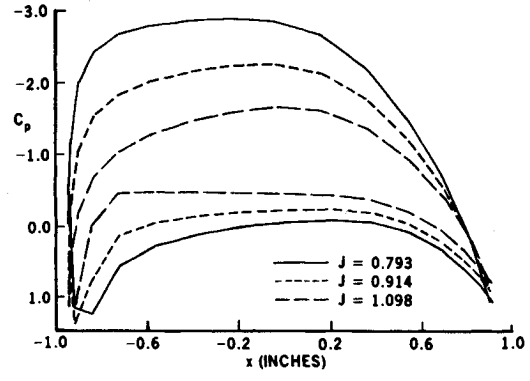

Fig. 13 Calculated pressure distributions on the aircraft propeller for $r/R=0.2$.

of attack and have no leading-edge pressure peaks. At any other advance ratio, $J=0.603$ in the present case, the blade operates at a different angle of attack and is bound to have a leading-edge peak on either the upper or lower surface. This is exactly the behavior predicted by the present method, but the vortex-lattice method fails to give a pressure peak at either ratio. The rather high negative peak predicted by the present method for $J=0.603$ appears to be real and demonstrates the superiority of the of the present method regarding pressure distribution. Essentially the same situation exists at the other radial locations.

To further verify the pressure distribution of Fig. 9, the blade section for $r/R=0.7$ was run as a two-dimensional airfoil at an angle of attack approximating $J=0.603$ in a conformal-mapping program,[7] which is known to give graphically exact potential-flow solutions. The results are shown in Fig. 10. All aspects of the panel-method pressure distribution are verified qualitively. Specifically, the conformal-mapping program gives: negative pressure maximum on the suction surface at 60% chord, crossing of suction- and pressure-surface pressures at about 10% chord, a steep negative leading-edge peak on what otherwise is the pressure surface, and small local peaks in the trailing-edge region on both surfaces due to flow acceleration around the rounded trailing edge. Due to the well-known three-dimensional relief, the two-dimensional pressure levels were somewhat higher, e.g., -0.25 in the midchord region instead of -0.20.

Tests of the aircraft propeller of Fig. 4 determined overall thrust and torque coefficients but not detailed pressure distributions.[8] Calculated and experimental thrusts, torques, and efficiencies are compared in Fig. 11 as functions of advance ratio. The results are very encouraging for a first calculation. The discrepancies between calculation and experiment at advance ratios greater than the design value $J=0.9$ are of the same sort obtained on wings and evidently are due to the loss of lift associated with viscous effects. This

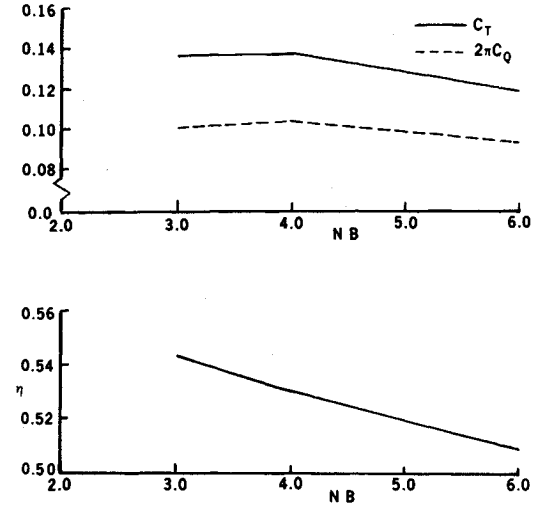

Fig. 14 Thrusts, torques, and efficiencies for the ship propeller with various blade numbers.

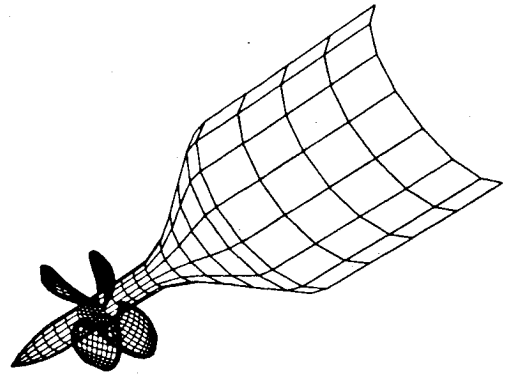

Fig. 15 Ship propeller on a large forebody.

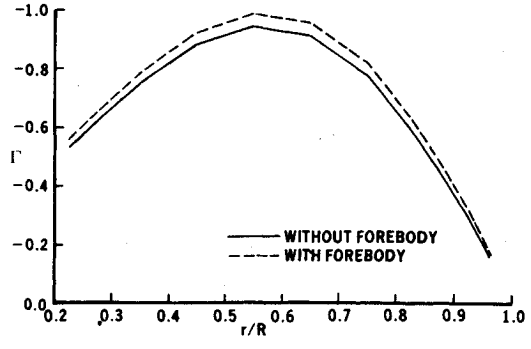

Fig. 16 Radial circulation distributions on the ship propeller with and without a forebody.

lift loss may be interpreted as a reduced effective angle of attack for wings or a modified blade pitch for propellers. At lower advance ratios, for which the blades are more heavily loaded, the use of the wake for the lightly loaded case probably would become less accurate. Possibly an improved wake geometry immediately downstream of the trailing edge would improve the results for these conditions. It is interesting to note that the errors in the calculated thrust and torque coefficients (too high in both cases) virtually cancel when their ratio is taken and the computed efficiency agrees very well with the experiments.

Other Calculated Results

Pressure distributions on the aircraft propeller at $r/R=0.7$ for various advance ratios are shown in Fig. 12. Figure 13 shows similar results for $r/R=0.2$. The curves of Fig. 12 are

typical of those obtained over most of the blade. However, the distributions on the inboard portions, as shown in Fig. 13, are quite different. The variation with J is as expected although there are no data for comparison. These pressures were normalized by freestream dynamic pressure, which explains the rather large values shown in the figure.

Calculations were performed for the ship propeller of Fig. 2 with three blades and six blades, as well as the four shown in the figure. As propeller theory indicates, the thrust, torque, and efficiency depend only weakly on blade number (Fig. 14), the loading on each blade being almost inversely proportional to blade number. Finally, the ship propeller was mounted on a rather large forebody (Fig. 15) intended to represent an extreme case of a torpedo. This had relatively little effect on flow conditions on the propeller, as can be seen from the calculated radial circulation distributions on Fig. 16.

Conclusion and Future Plans

The program described herein appears to be a valuable calculational tool for obtaining low Mach number flow about propellers. Results obtained using this method exhibit a level of detail previously unobtainable. Future work includes refinement of the wake model, generalization to the unsteady case, and incorporation of viscous effects.

References

[1]Hess, J.L., "The Problem of Three-Dimensional Lifting Flow and Its Solution by Means of Surface Singularity Distribution," *Computer Methods in Applied Mechanics and Engineering,* Vol. 4, Nov. 1974, pp. 283-319.

[2]Greeley, D. S. and Kerwin, J. E., "Numerical Methods for Propeller Design and Analysis in Steady Flow," *Transactions of SNAME,* Vol. 90, 1982.

[3]Byrd, P. F. and Friedman, M. D., *Handbook on Elliptic Integrals for Engineers and Physicists,* Springer-Verlag, Berlin, 1954.

[4]Hough, G. R. and Ordway, D. E., "The Generalized Actuator Disk," THERM Advanced Research Rept. TAR-TR6401, Therm, Inc., Itacha, NY, Jan. 1964.

[5]Blaisdell, G., Private Communication, Naval Ocean Systems Center, San Diego, CA.

[6]Kim, K. H. an Kobayshi, S., "Pressure Distribution on Propeller Blade Using Numerical Lifting-Surface Theory," *Proceedings of the SNAME Symposium—Propellers 84,* Virginia Beach, VA, May 1984.

[7]Halsey, D. N., "Conformal Mapping Analysis of Multielement Airfoils with Boundary-Layer Corrections," AIAA Paper 80-0069, Jan. 1980.

[8]Reid, E. G., "The Influence of Blade-Width Distribution on Propeller Characteristics," NACA TN 1834, March 1949.